

# Refined Tropospheric Delay Models for CONT11

D. Landskron · A. Hofmeister · J. Böhm

Received: date / Accepted: date

**Abstract** For the period of CONT11, a continuous VLBI campaign which lasted from September 15 through September 29, 2011, new  $a$  coefficients for the Vienna Mapping Functions 1 (VMF1, Böhm et al., 2006) and an extended calculation strategy for horizontal gradients were applied. The  $a$  coefficients of the mapping functions are usually calculated by ray-tracing through numerical weather models (NWM) from the European Centre for Medium-Range Weather Forecasts (ECMWF) with a spatial resolution of  $0.25^\circ \times 0.25^\circ$  every 6 hours. By enhancing the spatial resolution to  $0.125^\circ \times 0.125^\circ$  and using a new ray-tracing program called RADIATE, the actual refractivities are described in more detail. Moreover, existing equations for the calculation of the azimuth-dependent part of the slant delay by means of horizontal gradients were extended in order to achieve better accordance with the data from ray-tracing, which improves the resulting baseline length repeatabilities.

**Keywords** tropospheric delay · ray-tracing · VMF1 · horizontal gradients · GNSS · VLBI

---

Daniel Landskron  
Department of Geodesy and Geoinformation, Technische Universität Wien  
Gußhausstraße 27-29, 1040 Vienna, Austria  
Tel.: +43 (1) 58801 - 128 63  
E-mail: daniel.landskron@geo.tuwien.ac.at

Armin Hofmeister  
Department of Geodesy and Geoinformation, Technische Universität Wien  
Gußhausstraße 27-29, 1040 Vienna, Austria

Johannes Böhm  
Department of Geodesy and Geoinformation, Technische Universität Wien  
Gußhausstraße 27-29, 1040 Vienna, Austria

## 1 Introduction

Modeling tropospheric delays is one of the major error sources in the analysis of Global Navigation Satellite Systems (GNSS) or Very Long Baseline Interferometry (VLBI) observations. Many approaches like numerous mapping functions and several ways of handling the azimuthal asymmetry have been developed throughout the last decades; however, we are still far away from accuracies like 1 mm in position and 0.1 mm in velocity as requested by the Global Geodetic Observing System (<http://ggos.org>). For example, Böhm and Schuh (2001) tested spherical harmonics as supplement to mapping functions and gradients, Hobbiger et al. (2008) applied ray-tracing for precise point positioning in GPS, Geogout et al. (2011) developed so-called "adaptive mapping functions" to model azimuthal asymmetries, Zus et al. (2012) computed slant total delays in a numerical weather model, Nafisi et al. (2012) developed a ray-tracing program based on numerical weather models and Eriksson et al. (2014) investigated the impact of using ray-traced tropospheric delays on geodetic VLBI results.

In this paper, we compare ray-traced delays derived from operational analysis data of the European Centre for Medium-Range Weather Forecasts (ECMWF) with a spatial resolution of  $0.125^\circ \times 0.125^\circ$  every six hours against models usually applied for the reduction of tropospheric delays, such as the Vienna Mapping Functions (VMF1) and horizontal tropospheric gradients. In addition to the standard parameters, we also add specific VMF1 coefficients and gradients derived from the same ECMWF fields which are used for ray-tracing. Finally we assess the impact of the different approaches on geodetic parameters by analyzing the CONT11 dataset with the Vienna VLBI Software (VieVS, Böhm et al.,

2012) in terms of baseline length repeatability (BLR). For short time periods like CONT11, the BLR is simply the standard deviation of a set of measured baseline lengths.

## 2 Calculation of new mapping function coefficients

The Vienna Mapping Functions 1 (VMF1) for a certain elevation are based on the continued fraction form by Herring (1992):

$$\text{mf}(e) = \frac{1 + \frac{a}{1 + \frac{b}{1 + c}}}{\sin(e) + \frac{a}{\sin(e) + \frac{b}{\sin(e) + c}}} \quad (1)$$

where  $\text{mf}$  is the mapping function and  $e$  denotes the elevation angle. The coefficients  $b$  and  $c$  are determined by empirical functions as suggested by Böhm et al. (2006), whereas the coefficient  $a$  depends on the current weather situation. The VMF1 use ray-traced delays through a numerical weather model (NWM) with  $0.25^\circ \times 0.25^\circ$  spatial resolution as data input. The main outputs of ray-tracing are slant delays and zenith delays, with their ratio being the slant factor. Subsequently, the  $a$  coefficients can be determined from those delays and the values of VMF1 are provided online and in real-time on the GGOS Atmosphere server (<http://ggosatm.hg.tuwien.ac.at/DELAY/>). By means of ray-tracing (using the new ray-tracing program RADIATE (Hofmeister and Böhm, 2014)) through the currently available  $0.125^\circ \times 0.125^\circ$  NWM data, new values for the  $a$  coefficients could be obtained in a least squares approach.

Applying the re-calculated mapping function coefficients in VLBI analysis with VieVS slightly improves the resulting mean BLR from 1.09 to 1.08 cm. For 54% of the baselines (42 of 78), the BLR then is lower. Moreover it is notable, that when using the new coefficients, almost all repeatabilities of baselines containing station HOBART12 get by far better, while almost all repeatabilities of baselines containing station KOKEE get by far worse. This scenario also appears in investigations of BLR using different gradients (see section 3). The likeliest explanation for this is the geographic location of the VLBI station KOKEE. It is situated almost 1200 m above sea level on the island Kauai in the archipelago of Hawaii. The rapid altitude changes of the island together with the comparably low temporal resolution of

the NWM (6 hours) may not be suitable for properly representing the resulting changes in air refractivity, which contribute to the measured VLBI delays. The cause for the significantly better BLR of station HOBART12 on the island of Tasmania is still subject of investigation. However, when removing the stations HOBART12 and KOKEE from the solution, the general pattern of the results stays the same. That is, application of the re-calculated mapping function coefficients cause a general improvement of BLR, albeit only in the sub-mm range. Figure 1 shows the differences in BLR for all baselines.

Furthermore, the impact of choosing NWM with a spatial resolution of  $1^\circ \times 1^\circ$  was tested as well. However, as anticipated, the mean BLR gets slightly worse compared to the coefficients from the NWM with  $0.125^\circ \times 0.125^\circ$  spatial resolution (from 1.09 cm to 1.10 cm); For 59 % of the baselines (46 of 78), the BLR gets worse. Moreover, baselines containing station HOBART12 get considerably worse, while those containing KOKEE get slightly better.

## 3 Horizontal gradients

*It should be noted here that all BLR shown in this section used the standard VMF1 coefficients, not the re-calculated ones from the previous section.*

Applying mapping functions does not account for azimuthal asymmetries, which occur systematically on a large spatial scale due to the fact that the atmosphere is thicker at the equator and thinner at the poles and randomly on a small spatial scale, because the refractivity of the air varies with the azimuth because of changing weather conditions. Because the influence of azimuthal asymmetry increases with decreasing elevation angles, particularly all low-elevation observations require correction of this effect.

Applying horizontal gradients by using gradient formulas accounts for the bulk of this problem. At present, the gradient model by Chen and Herring (1997) is the most used and widely accepted way of modeling azimuthal asymmetries. It reads

$$\Delta L(a, e) = \underbrace{\Delta L_0(e)}_{\text{isotropic part}} + \underbrace{\text{mf}_g(e)[G_n \cos(a) + G_e \sin(a)]}_{\text{anisotropic part}} \quad (2)$$

with

$$\text{mf}_g(e) = \frac{1}{\sin(e) \tan(e) + 0.0032}$$

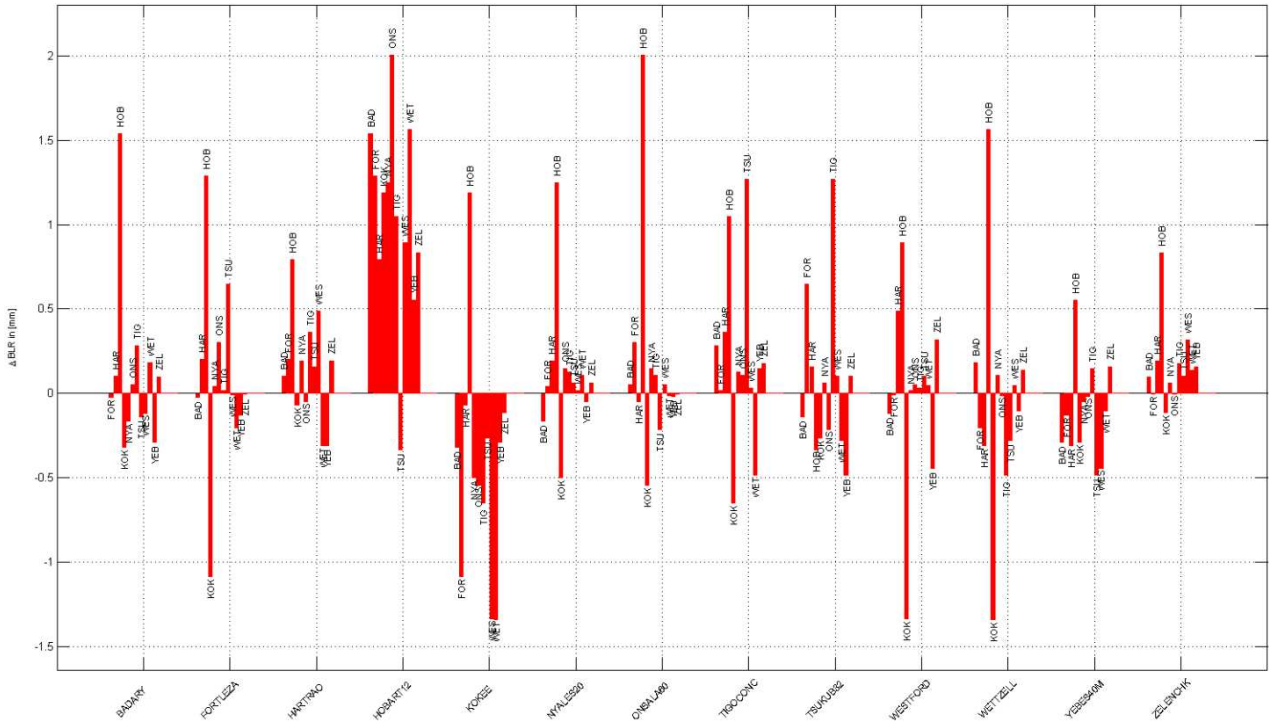


**Fig. 1** The differences in baseline length repeatabilities  $\Delta\text{BLR}$  between using the standard VMF1 coefficients and the re-calculated ones. All bars above the x-axis indicate that the repeatabilities of these baselines are lower for the re-calculated coefficients. Almost all bars above the x-axis with highest improvement correspond to baselines containing HOBART12, those below the x-axis with highest decline to KOKEE.

where  $a$  is the azimuth,  $e$  the elevation,  $L_0$  denotes the delay without horizontal gradients (product of the zenith delay and the mapping function) and  $G_n$  and  $G_e$  are the horizontal north and east gradients, respectively. Values for the horizontal gradients  $G_n$  and  $G_e$  depend on the time of the measurement and the location of the site. For example, gradients derived from horizontal gradients along the site vertical (Böhm and Schuh, 2007) can be downloaded from the GGOS Atmosphere server (<http://ggosatm.hg.tuwien.ac.at/DELAY/>). In this paper, we suggest adding higher order terms in azimuth to the expression in equation (2).

$$\begin{aligned} \Delta L(a, e) = \Delta L_0(e) + m f_g(e) [ & G_n \cos(a) + G_e \sin(a) \\ & + G_{n_2} \cos(2a) + G_{e_2} \sin(2a) ] \end{aligned} \quad (3)$$

and

$$\begin{aligned} \Delta L(a, e) = \Delta L_0(e) + m f_g(e) [ & G_n \cos(a) + G_e \sin(a) \\ & + G_{n_2} \cos(2a) + G_{e_2} \sin(2a) + G_{n_3} \cos(3a) + G_{e_3} \sin(3a) ] \end{aligned} \quad (4)$$

The horizontal gradients  $G_n$  and  $G_e$  and additional variables  $G_{n_2}$ ,  $G_{e_2}$ ,  $G_{n_3}$  and  $G_{e_3}$  were calculated in a

least squares adjustment using ray-traced tropospheric delays computed by the ray-tracing program RADIATE for each of the 14 stations and 60 epochs of CONT11. Therefore, 112 ray-traced delays at 16 evenly distributed azimuths ( $0 : 22.5 : 337.5$ ) and 7 elevations ( $3^\circ, 5^\circ, 7^\circ, 10^\circ, 15^\circ, 30^\circ, 70^\circ$ ) were used per station. The basic idea of the expansion of the gradient formula is that the oscillation of the systematic residual delays due to the shape of the Earth's atmosphere can be described more precisely, as is evident in figure 2. This figure shows the residuals between ray-traced slant delays and delays calculated by the 3 gradient formulas for station WESTFORD.

Calculating and averaging these ray-traced delay residuals for the testing period of CONT11 for all 14 CONT11 stations shows that they decrease by 69% when using equation (2), by 78% when using equation (3) and by 80% when using equation (4). This already shows a clear benefit of the revised gradient formulas.

Horizontal gradients as derived from ray-traced delays using NWM can be used as a priori gradients which serve as input to the VLBI analysis with VieVS. In addition, there is also the possibility of estimating the standard gradients (equation (2)) during the analysis itself, which is common practice. This is handled by

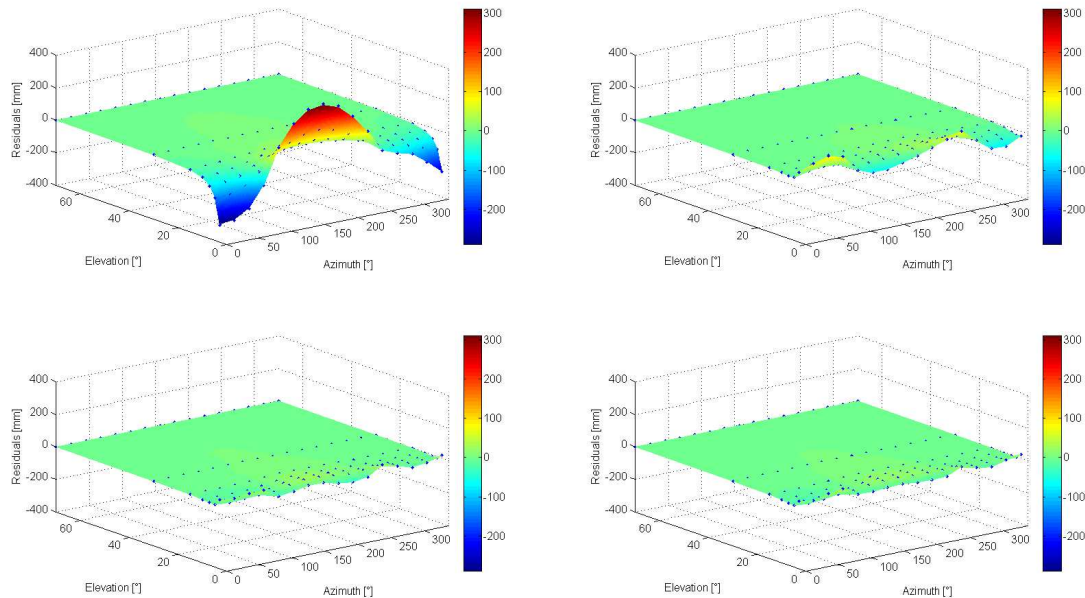


**Fig. 2** **Top left:** Residuals of the total slant delays for station WESTFORD at September 26, 2011, 18:00 GMT after subtraction of a mean over the 16 constantly distributed azimuths. The high residuals in north ( $a = 0^\circ$ ) and south ( $a = 180^\circ$ ) direction are mostly due to the high latitude location of the site, since the extension of the Earth’s atmosphere is higher at the equator and lower at the poles. **Top right:** Residuals after applying gradients by using equation (2); this lowers the residuals significantly. **Bottom left:** Residuals after applying gradients by using equation (3); again, the residuals are lowered considerably. **Bottom right:** Residuals after applying gradients by using equation (4); residuals hardly change compared to equation (3).

**Table 1** Mean BLR in [cm] for cases (a) standard gradients estimated during VLBI analysis using gradient formula (2) and (b) no gradients estimated during VLBI analysis. For reasons of interpolation, the time span was shortened to September 16 through September 28, 2011 here.

a priori gradients	(a)	(b)
none	1.07	1.20
using gradient formula (2)	1.05	1.10
using gradient formula (3)	1.03	1.09
using gradient formula (4)	1.04	1.09

a least squares adjustment using the standard gradient formula by Chen and Herring (1992). Table 1 shows the resulting mean BLR values for the different scenarios.

Table 1 reveals quite distinctively that if gradients calculated from ray-traced delays using NWM data with the revised gradient formulas (3) and (4) are used as a priori values, the resulting baselines have a slightly lower (better) mean BLR. Therefore, it is suggested that one use equation (3) for calculation of a priori gradients if the information is available. For 65% of the baselines (51 of 78), the BLR is lower compared to the standard gradient formula (2) (in case gradients are ad-

ditionally estimated in VLBI analysis). The additional gradient variables  $G_{n_2}$  and  $G_{e_2}$  can be provided in real-time in the same way as the gradients  $G_n$  and  $G_e$ ; thus, the download would not require additional work for the user.

As already mentioned before, north and east gradients are usually estimated in VieVS in a least squares adjustment using the normal gradient formula (2). It was also tested in this study whether the use of the two revised gradient formulas instead would bring a further improvement in BLR. That is, the additional gradient variables  $G_{n_2}$ ,  $G_{e_2}$ ,  $G_{n_3}$  and  $G_{e_3}$  were also estimated in the VLBI analysis. However, the resulting mean BLR thus increases considerably (in case of using no a priori gradients: 1.17 cm when using formula (3) and 1.22 cm when using formula (4), respectively). The reason for it is most likely that too many parameters are to be estimated which are highly correlated. In other words, there are not enough observations to properly de-correlate those parameters. As a result, gradients calculated by the extended gradient formulas presented in this paper can only be used as a priori gradients.

**Table 2** Mean BLR in [cm] for cases (a) gradients estimated during VLBI analysis using gradient formula (2) and (b) no gradients estimated during VLBI analysis. For reasons of interpolation, the time span was shortened to September 17 through September 27, 2011 here.

a priori gradients	(a)	(b)
none	1.07	1.20
APG	1.07	1.20
DAO	1.07	1.20

Lastly, the effect of using the empirical a priori gradients APG (Böhm et al., 2011) and DAO (Data Assimilation Office, GSFC, USA) was tested. As visible in table 2, their usage causes no detectable improvement in BLR.

## 4 Conclusions

Tested for the time period of VLBI campaign CONT11, a re-calculation of the VMF1 coefficients using ray-traced delays from a denser numerical weather model (NWM) with a resolution of  $0.125^\circ \times 0.125^\circ$  yields only a small improvement in mean BLR compared to the existing VMF1 coefficients (1.08 cm compared to 1.09 cm). This derivation of new coefficients is based on the new ray-tracing program RADIATE which will also be used to calculate ray-traced delays for the complete history of VLBI observations. Furthermore, revised gradient formulas based on that by Chen and Herring (1992) were studied. They yield slight improvements in BLR when used for the calculation of a priori gradients derived from ray-traced NWM delays. Hence, gradient formula (3) is suggested for use, if available. The BLR is reduced from 1.07 cm to 1.03 cm in the case that the standard gradients are additionally estimated in a least squares adjustment within the VLBI analysis and from 1.20 cm to 1.09 cm in the case of no subsequent estimation, respectively. Thus, another goal is to provide those gradients not only for the complete history of VLBI observations but also to reflect about strategies to provide gradients on global grids for the application in the analysis of GNSS observations.

**Acknowledgements** The authors would like to thank the Austrian Science Fund (FWF) for financial support of the project RADIATE VLBI (Ray-traced Delays in the Atmosphere for geodetic VLBI) (P25320) which is the basis of this work.

## References

1. Böhm J., Schuh H., Spherical Harmonics as a Supplement to Global Tropospheric Mapping Functions and Horizontal Gradients, Proceedings of the 15th Working Meeting on European VLBI for Geodesy and Astrometry, p. 143-148 (2001)
2. Böhm J., Werl B., Schuh H., Troposphere mapping functions for GPS and VLBI from ECMWF operational analysis data, *J. Geophys. Res.*, Vol. 111, B02406 (2006)
3. Böhm J., Schuh H., Troposphere gradients from the ECMWF in VLBI analysis, *J. Geod.*, Volume 81, Issue 6-8, pp 403-408 (2007)
4. Böhm J., Spicakova H., Urquhart L., Steigenberger P., Schuh H., Impact of A Priori Gradients on VLBI-Derived Terrestrial Reference Frames, in: Proceedings of the 20th Meeting of the European VLBI Group for Geodesy and Astrometry, March 29-30, 2011, ed. by W. Alef, S. Bernhart, A. Nothnagel, pp. 128-132 (2011)
5. Böhm J., Böhm S., Nilsson T., Pany A., Plank L., Spicakova H., Teke K., Schuh H., The new Vienna VLBI Software VieVS, in: Proceedings of IAG Scientific Assembly 2009, International Association of Geodesy Symposia Series Vol. 136, edited by S. Kenyon, M. C. Pacino, and U. Marti, p. 1007-1011, (2012)
6. Chen G., Herring T.A., Effects of atmospheric azimuthal asymmetry on the analysis of space geodetic data, *J. Geophys. Res.*, Vol. 102, No. B9: 20,489 – 20,502 (1997)
7. Eriksson D., MacMillan D. S., Gipson J. M., Tropospheric Delay Raytracing Applied in VLBI Analysis, *J. Geophys. Res. Solid Earth*, 119 (2014)
8. Gegout P., Biancale R., Soudarin L., Adaptive mapping functions to the azimuthal anisotropy of the neutral atmosphere, *J. Geod.*, 85:661–677 (2011)
9. Herring T.A., Modeling atmospheric delays in the analysis of space geodetic data, in: Publications on Geodesy, Vol. 36, Proceedings of Refraction of Transatmospheric Signals in Geodesy, edited by J. C. DeMunck and T.A. Th. Spoelstra, pp. 157-164, Netherlands Geodetic Commission Publications in Geodesy (1992)
10. Hobiger T., Ichikawa R., Takasu T., Koyama Y, Kondo T., Ray-traced troposphere slant delays for precise point positioning, *Earth Planets Space*, 60, e1-e4 (2008)
11. Hofmeister A., Böhm J., Ray-traced Delays in the Atmosphere for Geodetic VLBI, IVS 2014 General Meeting Proceedings, ed. by D. Behrend, K.D. Baver, and K. Armstrong (2014)
12. Nafisi V., Madzak M., Böhm J., Ardalan A. A., Schuh H., Ray-traced tropospheric delays in VLBI analysis, *Radio Science*, Vol. 47, RS2020 (2012)
13. Nilsson T., Böhm J., Wijaya D.D., Tresch A., Nafisi V., Schuh H., Path Delays in the Neutral Atmosphere. In: Böhm J., Schuh H. (eds): Atmospheric Effects in Space Geodesy. Springer Verlag, ISBN: 978-3-642-36931-5 (2013)
14. Zus F., Bender M., Deng Z., Dick G., Heise S., Shang-Guan M., Wickert J., A methodology to compute GPS slant total delays in a numerical weather model, *Radio Science*, Vol. 47, RS2018 (2012)